



The contrasting climate response to tropical and extratropical energy perturbations

Matt Hawcroft¹ · Jim M. Haywood^{1,2} · Mat Collins¹ · Andy Jones²

Received: 20 April 2017 / Accepted: 8 January 2018
© The Author(s) 2018. This article is an open access publication

Abstract

The link between cross-equatorial energy transport, the double-intertropical convergence zone (DI) problem and biases in tropical and extratropical albedo and energy budgets in climate models have been investigated in multiple studies, though DI biases persist in many models. Here, a coupled climate model, HadGEM2-ES, is used to investigate the response to idealised energy perturbations in the tropics and extratropics, in both the northern and southern hemispheres, through the imposition of stratospheric aerosols that reflect incoming radiation. The impact on the tropical climate of high and low latitude forcing strongly contrasts, with large changes in tropical precipitation and modulation of the DI bias when the tropics are cooled as precipitation moves away from the cooled hemisphere. These responses are muted when the extratropics are cooled, as the meridional energy transport anomalies that are excited by these energy budget anomalies are partitioned between the atmosphere and ocean. The results here highlight the persistence of the DI bias in HadGEM2-ES, indicating why little progress has been made in rectifying these problems through many generations of climate models. A highly linear relationship between cross-equatorial atmospheric energy transport, tropical precipitation asymmetry and tropical sea surface temperature biases is also demonstrated, giving some suggestion as to where improvements in these large scale, persistent biases may be achieved.

Keywords Climate models · Energy transport · ITCZ · Tropics · Extratropics

1 Introduction

Many studies have been devoted to relating large-scale biases in tropical precipitation, particularly the mean latitude of the intertropical convergence zone (ITCZ), often referred to as the 'double ITCZ' (DI) problem, to biases elsewhere in climate models. These studies have evaluated the controls on tropical precipitation in simplified frameworks, such as mixed layer/slab ocean (e.g. Chiang and Bitz 2005; Kang et al. 2008; Frierson and Hwang 2012; Cvijanovic and Chiang 2013) or aquaplanet (e.g. Voigt et al. 2014a, b) experiments, through to several recent studies using fully-coupled global climate model (GCM) simulations (e.g. Deser et al. 2015; Haywood et al. 2016; Kay et al. 2016; Tomas et al.

2016; Hawcroft et al. 2016; Mechoso et al. 2016; Stephens et al. 2016).

It has been shown that biases in the top of atmosphere (TOA) radiation budget, such as the representation of the observed hemispheric albedo symmetry (Voigt et al. 2014b; Loeb et al. 2015), may lead to biases in cross-equatorial energy transport (e.g. Haywood et al. 2016; Kay et al. 2016; Hawcroft et al. 2016). Further, the cross-equatorial atmospheric energy transport has been related theoretically (e.g. Bischoff and Schneider 2014, 2016), in observations (e.g. Schneider et al. 2014) and in GCM simulations (e.g. Hwang and Frierson 2013; Loeb et al. 2015) to the zonal mean ITCZ location. The ITCZ moves towards the warmer hemisphere as atmospheric energy transport increases out of that hemisphere. As such, large scale biases in TOA energy budgets can have a significant impact on tropical precipitation.

Several of the fully-coupled GCM studies focus on the impact of biases (and perturbations) to the extratropical energy budget to investigate the tropical response to changes in Arctic sea ice extent (Deser et al. 2015; Tomas et al. 2016) or to reducing the long-standing bias in Southern Ocean albedo in coupled models (Kay et al. 2016; Hawcroft et al.

✉ Matt Hawcroft
m.hawcroft@exeter.ac.uk

¹ College of Engineering, Mathematics and Physical Sciences, University of Exeter, Exeter, UK

² Met Office Hadley Centre, Exeter, UK

2016; Mechoso et al. 2016), which is known to be related to inadequate simulation of observed cloud cover and cloud properties (Bodas-Salcedo et al. 2014). When perturbing the extratropical energy budget in a coupled simulation, the tropical atmospheric response is modulated by the fractional change in total meridional energy transport between the atmosphere and ocean. If much of the energy transport response in the near equatorial region occurs in the ocean, the tropical atmosphere response may be muted. By contrast, a larger meridional energy transport response in the tropical atmosphere may lead to corresponding adjustments in tropical precipitation.

It is also not clear that an equal perturbation that is applied to the northern and southern hemisphere extratropics would have an equivalent (though antisymmetric) response in the tropics. In terms of energy transport, the coupled experiments discussed in Deser et al. (2015) and Tomas et al. (2016) exhibit much of their energy transport response in the Atlantic, as the Meridional Overturning Circulation (AMOC) responds to a warming of the high latitudes from sea ice loss, but those experiments also realised a northward migration of the ITCZ related to increased atmospheric energy transport through the tropics. In contrast, Kay et al. (2016) and Hawcroft et al. (2016) found much of the energy transport response to a cooling of the Southern Ocean to be in the Pacific Ocean, with relatively little change in tropical atmospheric energy transport and a muted ITCZ response. Mechoso et al. (2016), applying a forcing between 30–60S in two models, found very little ITCZ response in NorESM but a northward shift of the ITCZ in the UCLA GCM. Some of these differences are likely associated with differing model background states and biases, but may also be associated with experimental design. This issue is further discussed in Sect. 3.8 and the spread of model response warrants further investigation.

In the tropics, given the demonstrated relationship between cross-equatorial energy transport and the DI problem, and also the persistence of the DI biases through generations of GCMs, it is of interest to evaluate the tropical precipitation response to qualitatively similar perturbations applied in the tropics and extratropics, and also in the northern and southern hemispheres. It has been argued that many biases in tropical precipitation may be associated with such issues as inadequate convection parameterisation, convective-dynamical coupling and ocean-atmosphere coupling (e.g. Zhang and Wang 2006; Lin 2007; Bellucci et al. 2010; Oueslati and Bellon 2015), implying the DI problem may be of tropical origin. Evaluating the response to both tropical and extratropical perturbations in a model where the physics remain consistent is one approach to untangling causality in this issue.

In this study, we apply simplified perturbations to the energy budget of a GCM, HadGEM2-ES, the coupled

atmosphere-ocean Earth system model of the Met Office Hadley Centre (Collins et al. 2011). HadGEM2-ES has been shown to accurately reproduce global observed surface temperature change (Collins et al. 2011) and exhibits biases in the patterns of TOA shortwave and longwave radiation biases that are comparable to many other state-of-the-art GCMs, including those related to excessive precipitation in the southern tropics (Li et al. 2013). Two previous studies using HadGEM2-ES inform the present work. In Haywood et al. (2016), the whole southern hemisphere of HadGEM2-ES was brightened in order to replicate the observed symmetry of hemispheric albedo via adjustments to either stratospheric aerosol optical depth, ocean albedo or cloud droplet number concentration, with improvements in tropical precipitation observed in all cases. In Hawcroft et al. (2016), the southern hemisphere albedo was increased via targeted adjustments to the Southern Ocean (where much of the mean hemispheric bias is generated), yet did not yield improvements to tropical precipitation due to the modulation of the model response by the ocean-atmosphere energy partitioning, discussed above, as changes in total energy transport in the tropics largely occurred in the ocean. We extend the approach of these studies here by applying idealised stratospheric aerosol loadings to the model in latitudinal bands of equal area to explore the differential response to both tropical and extratropical and northern and southern hemisphere perturbations. The intention of these simulations is to evaluate the spread of response in tropical precipitation and to identify the causes and teleconnections which characterise these differences. In doing so, an increased understanding of the likely routes to improving tropical precipitation biases in GCMs may be gained. Further insights into the dependence of the results of previous studies, using HadGEM2-ES and other models, to their experimental design may also be achieved.

In Sect. 2 the model and experimental set-up is described, along with the observational datasets used to constrain the model. In Sect. 3 the results of the experiments are discussed. The findings, limitations and implications of the study are summarised in Sect. 4.

2 Data and methods

2.1 HadGEM2-ES climate model

HadGEM2-ES (Collins et al. 2011) is a fully coupled atmosphere-ocean climate model developed by the Met Office Hadley Centre. The atmospheric component has 38 levels extending to 40 km, with a horizontal resolution of $1.875^\circ \times 1.25^\circ$ in longitude and latitude, respectively, equivalent to a surface resolution of about $200 \text{ km} \times 140 \text{ km}$ at the Equator, reducing to $120 \text{ km} \times 140 \text{ km}$ at 55° latitude. ES

refers to the Earth System version, which includes coupling to a tropospheric chemistry scheme, the terrestrial carbon cycle and an ocean biogeochemistry scheme. The oceanic component has 40 unevenly spaced vertical levels and a latitude–longitude grid with a zonal resolution of 1° globally and meridional resolution of 1° poleward of 30°N/S , which increases smoothly from 1° at 30°N/S to $1/3^\circ$ at the equator.

2.2 Experimental design

In this study, we perturb the energy budget in the tropics and extratropics in both the northern and southern hemispheres. Informed by the approaches in Haywood et al. (2016) and Hawcroft et al. (2016), discussed above, and in order to provide a perturbation that is comparable across the experiments, we impose idealised perturbations to stratospheric aerosol optical depth in four separate bands, shown in Fig. 1a—the northern hemisphere extratropics (90N – 30N , NET) and tropics (30N – 0 , NT) and the southern hemisphere extratropics (30S – 90S , SET) and tropics (0 – 30S , ST). These bands have equal area and the aerosol optical depth is adjusted equally in all regions. We acknowledge that this methodology does not provide equivalent perturbations to the Earth’s energy budget in each case, but we diagnose the magnitude of the perturbations via the commonly used ‘Effective Radiative Forcing’ approach (Stocker (2014), see Sect. 3.3), and further note that we are most interested in the patterns of response rather than their absolute magnitude. We compare these simulations to a control experiment which has a globally uniform, negligible stratospheric aerosol loading of 0.02 AOD (‘NoAero’). All simulations are run with present day forcings and are branched at the same date from a control experiment which includes observed, historical aerosol forcings. Three experiments with different AOD perturbations are performed for each band, giving a total of 12 experiments plus the NoAero control case. Based on the maximum loadings of major observed eruptions (e.g. Pinatubo, El Chichon, Krakatoa), where equivalent bands to those used in these experiments peaked in the range of 1.5–2 AOD, we apply perturbations of 1, 2 and 4 AOD in each band with 0.02 applied across the rest of the model stratosphere. These forcings broadly equate to half/one/two times the maximum load over the equivalent area from any observed eruption (see Sato et al. 1993, and updated data). Given the climate impacts of these observed events (e.g. Hofmann 1987; Hansen et al. 1992; Robock 2000), forcings of these magnitudes are expected to induce discernible responses in the model climate, particularly in the 4AOD case.

To observe a full, equilibrium response to any large perturbation in the energy budget of a model may take hundreds of years, due to the timescale on which the deep ocean energy balance and transport may adjust. Here we focus on

the near term, faster response where we show the first two decades of data from each experiment. For the 4AOD and NoAero cases, the simulations are extended to 80 years, confirming that the qualitative response observed in the first two decades is representative of the response at this longer timescale, particularly with respect to the large-scale features which are the focus of this study. In Hawcroft et al. (2016), a subset of experiments were extended to 100 years and in Kay et al. (2016), where the Southern Ocean was perturbed in the CESM GCM, experiments were run for 200 years. In both cases, the fast response was also found to be qualitatively similar to the longer term response. For the effective radiative forcing (ERF) calculations shown in Table 1 and discussed in Sect. 3.3, fixed SST simulations are run for 10 years, which is sufficient time for the atmosphere to respond to the imposed forcing in order to calculate the ERF in each experiment.

Ocean heat transport is calculated explicitly in HadGEM2-ES. Atmosphere heat transport is calculated as the difference between the top of atmosphere and surface fluxes at each latitude, which is then integrated from the south to north pole. The total energy transport is the sum of the two and the energy transport budget is closed at the north pole (see, for example, Fig. 7). Given these experiments are not in equilibrium, if the total energy transport was calculated solely from the top of atmosphere fluxes, the energy budget would not be closed (see Hawcroft et al. 2016, for further details).

2.3 Observational datasets

The primary focus of this study is on the nature of the model response to perturbations. As such, observations are shown to provide a familiar reference state to the reader. TOA and surface radiative fluxes are obtained from the CERES (Wielicki et al. 1996) Energy Balanced and Filled (EBAF) Ed2.8 product (Loeb et al. 2009, 2012; Kato et al. 2013). Meridional energy transports are calculated using CERES TOA fluxes, combined with total atmospheric heat tendency and divergence estimates from the ERA-Interim (Dee et al. 2011) dataset (see Loeb et al. 2015), which are obtained from NCAR (2014), and total ocean heat tendencies from

Table 1 Global mean top of atmosphere net radiation anomalies (W m^{-2}) in the 4AOD experiments (Coupled), with corresponding values for fixed SST experiments (Fixed) compared to NoAero control simulations performed in a coupled/fixed SST framework

Experiment	NET	SET	NT	ST
TOA Net radiation anomalies				
Coupled	– 0.68	– 1.06	– 0.46	– 0.52
Fixed	– 0.68	– 1.29	– 1.42	– 1.81

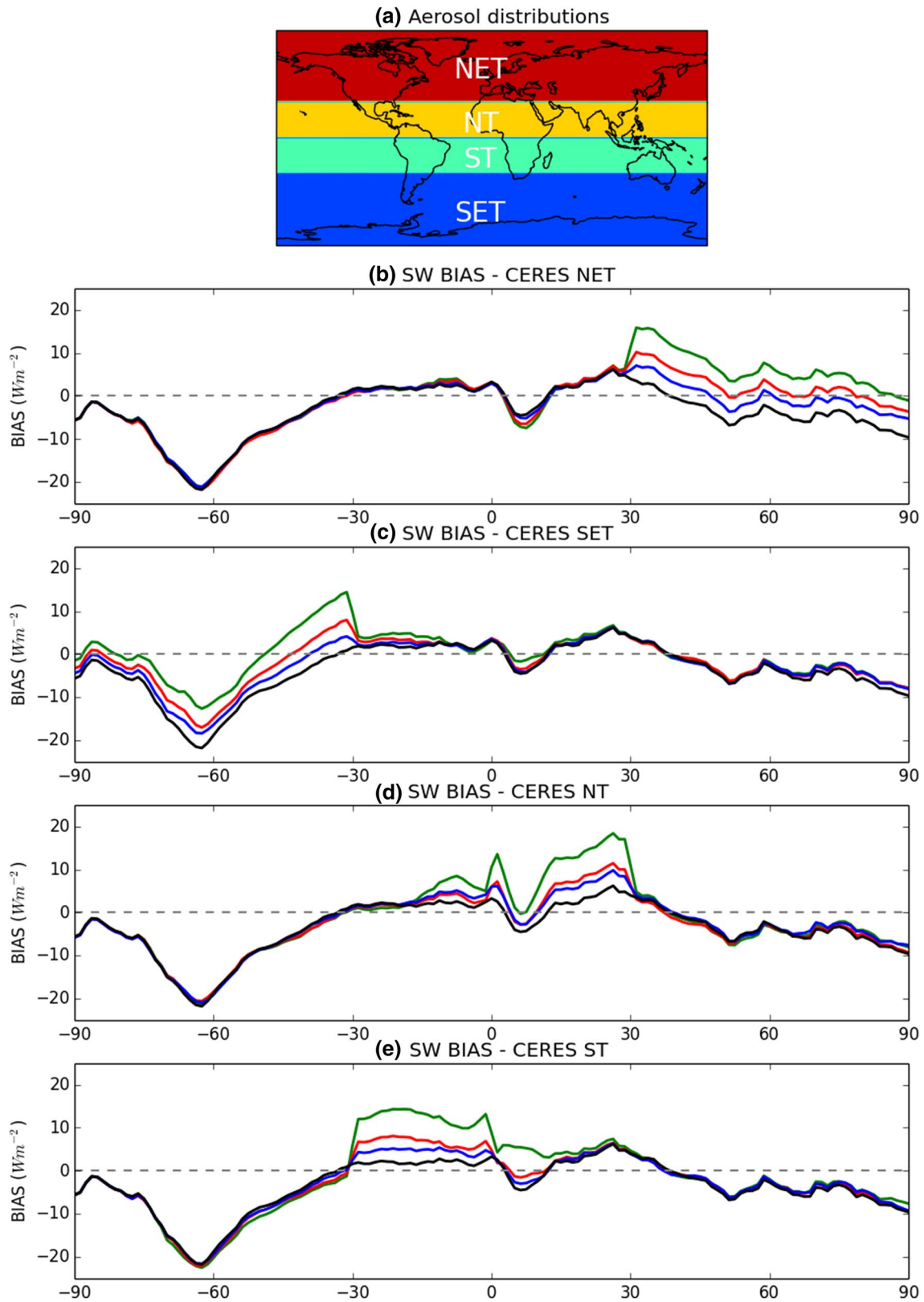


Fig. 1 a The distribution of stratospheric aerosol optical depth applied in the experiments. Each of the bands is perturbed in a separate experiment, with a background 0.02 AOD applied in the other three bands. **b–e** zonal mean TOA shortwave radiation biases (W

m^{-2} , upwards as positive) relative to CERES shown for each set of experiments. The black line shows the NoAero simulation with the blue, red and green lines showing the 1, 2 and 4AOD experiments, respectively

the ORAS4 dataset (Balmaseda et al. 2013). Data is obtained from 2003–2013 and full details of the data and method of calculation are given in Hawcroft et al. (2016). Precipitation estimates are obtained from the Global Precipitation Climatology Project (GPCP) version 2.2 data (Adler et al. 2003) over the period 1979–1998. Sea surface temperatures are obtained from the NOAA Optimum Interpolation Sea Surface Temperature (OISST) version 2 data over the period 1981–2013 (Reynolds et al. 2007; Reynolds 2009). Net surface flux data is from the OAFflux dataset from 1983–2009 (Yu et al. 2008) and is ocean only.

3 Results

3.1 TOA energy balance

In Fig. 1b–e the TOA shortwave radiation biases are shown for each experiment. The climatological bias in the Southern Ocean is clear in the NoAero experiment and is comparable to HadGEM2-ES's historical simulations (see Hawcroft et al. 2016). Whilst we have noted that the forcings between the NET, SET, NT and ST experiments may not be equivalent (see Table 1), those applied in the 1, 2 and 4AOD experiments, if the model response is linear, should approximately double from each experiment to the next. In the NET and SET experiments this appears to be largely true, at least in the region where the forcings are applied, though with some differences in the tropics indicating that the extratropical-tropical teleconnections may not scale with forcing (in particular near 10N, where the core of the northern hemisphere ITCZ is located). The response to the NT and ST experiments suggest that there are non-linearities in the tropical circulation response to forcings, with relatively modest changes from 1AOD to 2AOD and larger responses from the 2AOD to 4AOD experiments.

3.2 Precipitation

The zonal mean precipitation response is shown in Fig. 2. It is first worth noting the DI bias in the model, with a peak in precipitation around 10S which is greatly overestimated relative to observations. The far greater response to the tropical (NT and ST compared to NET and SET) forcing is readily apparent. The tropical precipitation response to extratropical forcing further indicates that the teleconnections from the extratropics-tropics are not linear. In the NET case (Fig. 2b), very little change in tropical precipitation occurs for the 1AOD experiment and for the SET case (d), the response to 1AOD and 2AOD are similar and muted when compared to 4AOD. In the two tropical cases, NT (f) and ST (h), the scaling of the precipitation to the AOD increase is more linear.

3.3 Effective radiative forcing

It is worth contextualising the magnitude of the response in each experiment by examining the changes in net TOA radiation in comparison to calculations of effective radiative forcing (ERF) obtained from experiments performed with fixed SSTs. The ERFs are intended to provide an indication of the direct response to the forcing, without the significant reorganisations of ocean and atmospheric circulation which occur in the coupled experiments, and therefore the energy perturbation that is associated with the aerosol itself. Table 1 provides global TOA anomalies for the 4AOD simulations and equivalent figures for experiments run with fixed SSTs. In the latter experiments, the reorganisation of the climate system seen in the coupled experiments is highly damped (not shown). The damping of the circulation response in the ERF experiments is related to surface fluxes—in the fixed SST cases, the ocean surface provides a reservoir of energy to compensate the cooling in each latitude band, bringing the atmosphere back towards equilibrium. In contrast, in the coupled cases the ocean surface only provides partial compensation, with dynamical changes in the atmosphere serving to import further energy into the atmosphere of the cooled region.

The ERF in the NET experiment is substantially smaller than in the other three experiments, explicable by the lower insolation in the higher latitudes and the large expanses of land areas with higher reflectance in the northern hemisphere extratropics. In contrast, the SET experiment has an ERF almost twice the magnitude (-1.29 against -0.68 Wm^{-2}) since the southern ocean has much lower albedo. It might therefore be expected that the response in SET would be substantially larger than in NET. Both the tropical experiments, NT and ST, have higher ERFs (-1.42 and -1.81 Wm^{-2} , respectively). These energy budget changes are strongly modulated by the dynamical response in the coupled simulations, such that the net TOA anomaly in the SET coupled experiment is approximately double that of the NT and ST experiments. The coupled response is in large part associated with dynamical changes in the model induced by the aerosol forcing, rather than the forcing itself—the equivalent to climate feedbacks in climate sensitivity experiments (e.g. Gregory et al. 2004). In spite of the very different ERFs, the first-order dynamical response of the SET and NET 4AOD experiments is similar in magnitude (Fig. 2) and is far greater in ST and NT than SET in spite of the ERFs being 10 and 40% higher and the net TOA response in the coupled experiments being less than half (Table 1) that in the SET experiment. This emphasises the potential sensitivity of model behaviour to the latitude at which any forcing is applied or, in the context of model evaluation, any net radiation bias may occur.

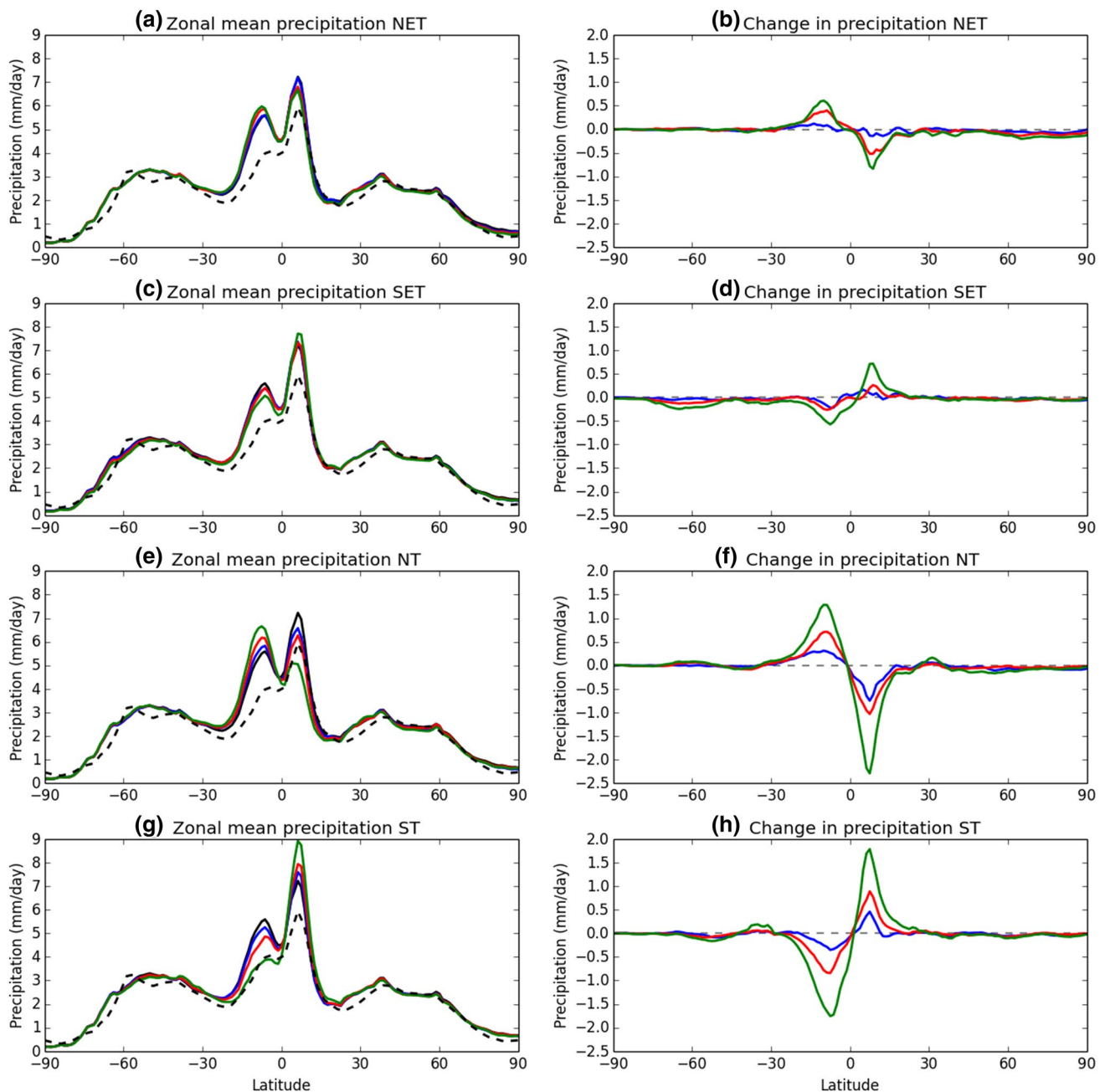


Fig. 2 Zonal precipitation (mm day^{-1}) in NoAero (black) and the 1AOD (blue), 2AOD (red) and 4AOD (green) experiments, with GPCP (dashed black, **a, c, e, g**) and anomalies from the NoAero experiment to the 1/2/4AOD experiments (**b, d, f, h**)

3.4 Albedo

Previous studies have shown the strong relationship between cross-equatorial energy transport and tropical precipitation/the DI problem and this has further been linked to asymmetries in inter-hemispheric albedo (e.g. Hwang and Frierson 2013; Bischoff and Schneider 2014; Schneider et al. 2014; Loeb et al. 2015; Bischoff and Schneider 2016).

In Fig. 3 global and hemispheric mean albedo and net TOA radiation is shown. In all experiments, albedo and outgoing TOA net radiation is increased (black lines in a and b, figures in Table 1) as the stratospheric aerosol reflects incoming radiation. This directly changes the albedo in the hemisphere where the aerosol is imposed, but has further implications for both albedo and TOA radiation through the changes to the model climate induced by the perturbations to the energy budget. Figure 3 shows that the global albedo

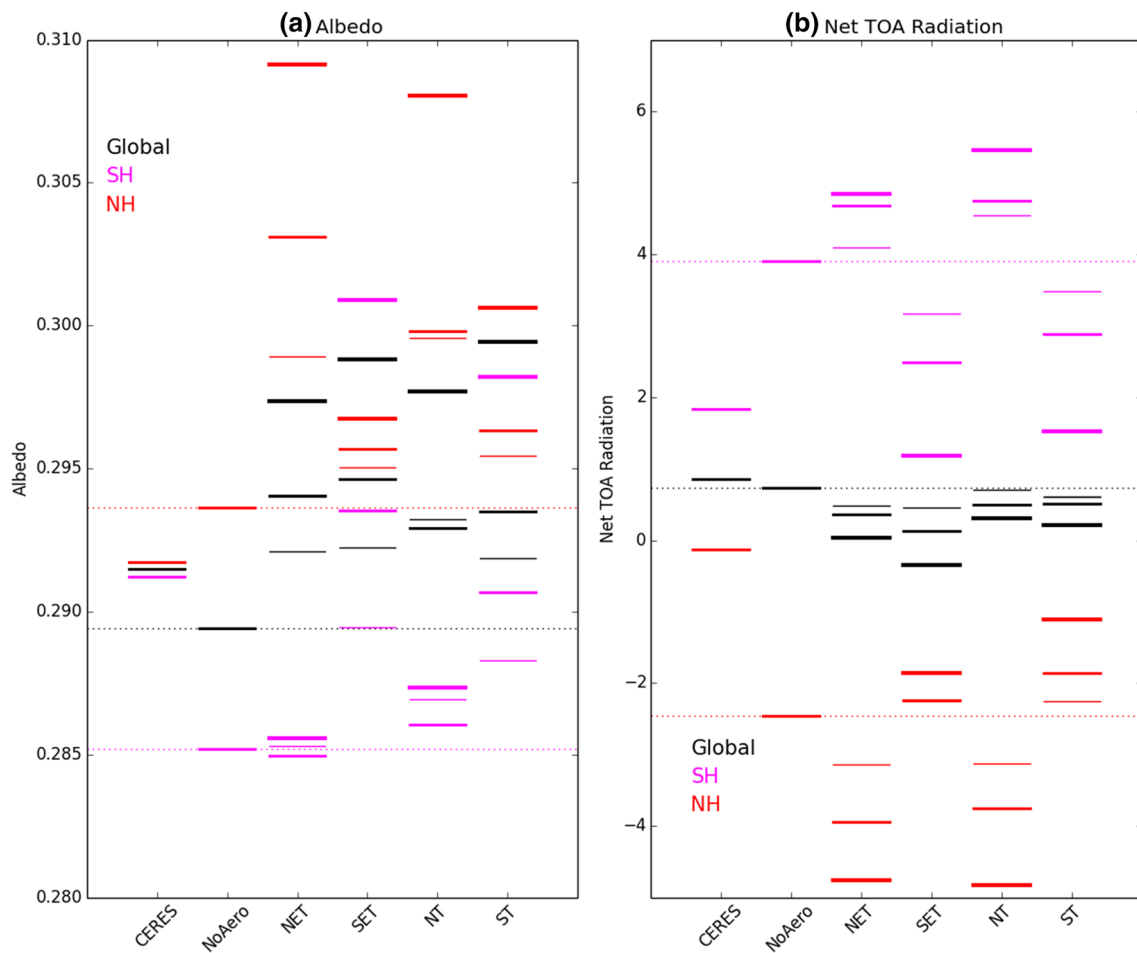


Fig. 3 **a** Hemispheric mean albedo in the southern (magenta) and northern (red) hemispheres in CERES, the NoAero experiment and the four perturbed experiments and **b** TOA net radiation ($W m^{-2}$, downwards as positive) globally (black) and in the southern

(magenta) and northern (red) hemispheres, for the same datasets. In the experiments, the thinnest line shows the 1AOD case, the medium thickness line the 2AOD case and the thickest line the 4AOD case. The dotted lines extend the NoAero results to aid interpretation

changes (at least for the 4AOD experiments) are greater in the two southern hemisphere experiments, SET and ST, compared to NET and NT. In contrast, the response in global TOA net radiation (black lines in b, figures in Table 1) is less pronounced in the NT than ST experiments compared to the NET and SET experiments, in spite of the incoming radiation being greater in the tropics. The reasons for these differences are a combination of the location of the forcings being applied and the climate response in each experiment.

In the SET and NET experiments, the albedo changes are comparable in the high latitudes (Fig. 1b, c) but the response in the tropics in the SET experiment leads to higher global mean albedo. In the ST and NT experiments, both lead to a redistribution of precipitation into the opposite hemisphere (Fig. 2f, h), though the spatial distribution of these changes are material to the TOA radiative response. Figure 4 shows precipitation for the NoAero experiment and anomalies to the 4AOD experiments. In the ST case (e), precipitation is

intensified/reduced in the northern/southern tropics and the opposite in the NT case (d), though the distribution of these changes and the associated cloud distributions gives a stronger response in the hemispheric and global mean in the ST case. The TOA radiation changes (Fig. 3b) are the result of a balance in shortwave and longwave fluxes associated with both the direct impact of the aerosols and the distribution (and height) of clouds.

In the ST and NT cases, there are comparatively larger changes in the tropical atmosphere and precipitation (Figs. 2f, h and 4d, e) and in the location of the deep, cold topped convective clouds that produce much of this precipitation. Given the tropics have warm underlying surfaces this means that in the NT and ST cases, the global net TOA radiation changes are smaller as the shortwave and longwave effects offset each other. This occurs in spite of the fact the changes in each hemisphere are greater (Fig. 5e–h), with the interhemispheric contrast reduced in ST and increased in NT

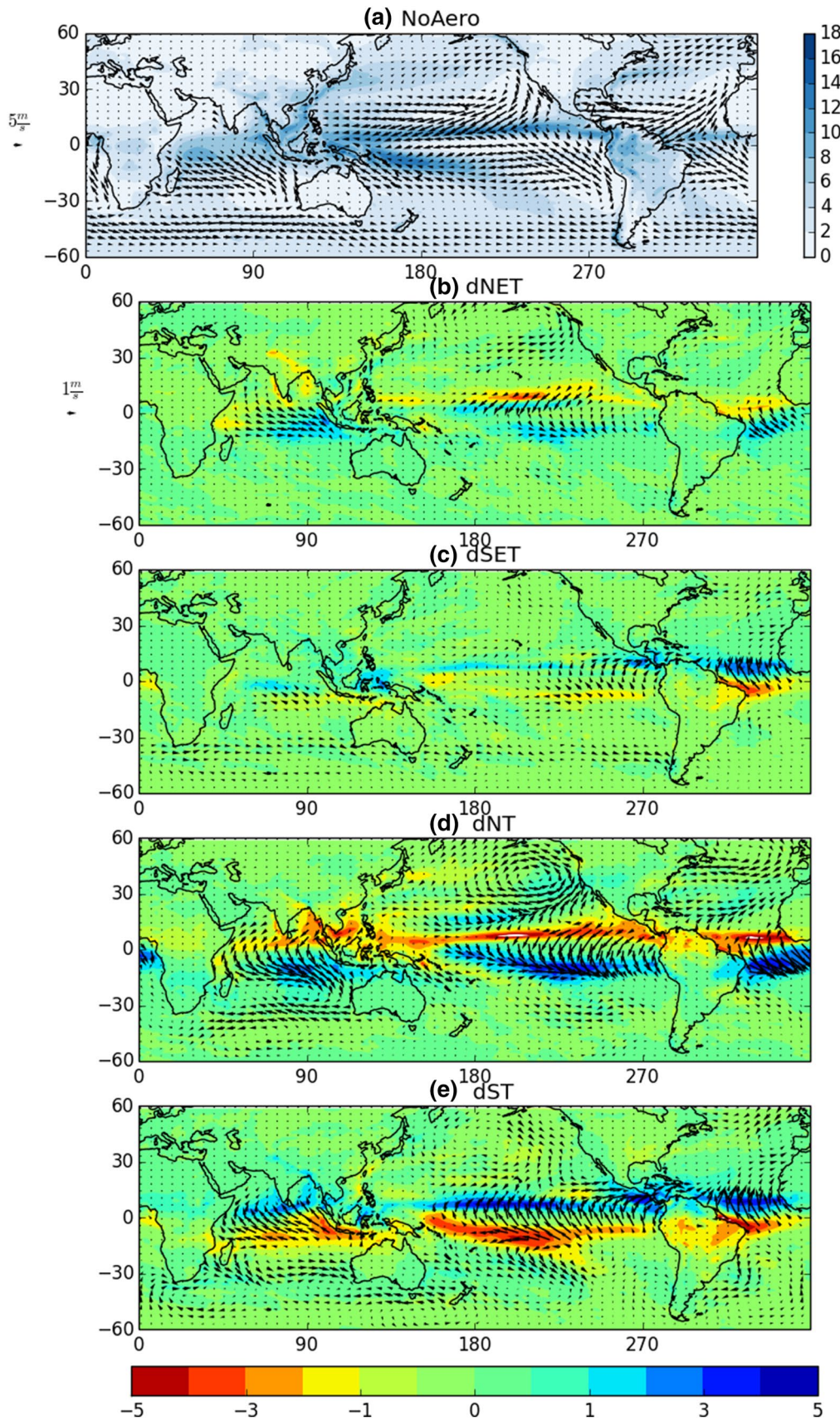


Fig. 4 **a** Annual mean precipitation (mm day^{-1}) and 1000 hPa wind vectors for the NoAero experiment and **b–e** precipitation and wind anomalies for the 4AOD experiments

(Fig. 3b). In the NET and SET cases, the smaller changes in atmospheric circulation and tropical precipitation (Figs. 2b, d, 4b, c) mean the increase in outgoing radiation associated with the forcing is not offset by a compensating change in the tropics of the opposing hemisphere (Fig. 5a–d). The simple hemispheric and global mean metrics are a function of complex reorganisations of the model climate in each case and demonstrate that the latitudinal distribution of perturbations, or comparable model biases, may have substantially different impacts on the tropical climate in a model.

3.5 Cross-equatorial energy transport

Given hemispheric asymmetries in net TOA radiation govern the energy balance between the hemispheres, we now turn to the related metric of cross-equatorial energy transport (CET, Fig. 6). The expected relationship between cooling in one hemisphere and an increase in total (atmospheric and ocean) energy transport into that hemisphere is observed, with increased northward energy transport in both NT and NET and southward anomalies in ST and SET. The greater changes are in the two tropical experiments, since in spite of the larger changes in global net TOA radiation in the extratropical experiments (Fig. 3 and Table 1), it is the difference between the two hemispheres that is associated with CET. Given the tropical and extratropical forcings are of similar magnitude, this indicates that adjustments in circulation and energy transport efficiency (e.g. via the extratropical storm tracks) modulate the extratropical-tropical teleconnection, reducing the impact at the equator in NET and SET. It is of interest to note that the ST 4AOD experiment results in CETs which are comparable to observations—in other words, in order to correct the error in model CET, a perturbation equivalent to two Pinatubo eruptions is required, underlining how persistent this error is and going some way to explaining why DI errors (which have been related to atmospheric CET errors in several studies) have been persistent through generations of climate models (see, e.g. Hwang and Frierson 2013; Loeb et al. 2015).

At the equator, the total CET adjustment in the NT and ST cases can be seen to broadly scale with the magnitude of the forcing, whereas this is not the case for the NET and SET cases. For example, very little change in CET is observed in the NT 1AOD case, which reconciles with the small change in tropical precipitation in that simulation (Fig. 2b, blue line) compared to the 2AOD and 4AOD cases, suggesting some non-linearity in the response of the model. In the SET case, though the total CET adjustments in the 1AOD and 2AOD experiments are similar, it is notable that the ocean

CET changes little from 1AOD to 4AOD, with the increased southward anomaly primarily occurring in the atmosphere. Again, this can be associated with the tropical precipitation anomalies in those experiments (Fig. 2d). In the ST and NT cases, the split between ocean and atmosphere of the total CET response is non-monotonic, but the broad linearity of the total response is apparent and the changes in atmospheric CET can be related to the changes in tropical precipitation.

3.6 Meridional energy transport

Expanding the evaluation of the energy transport response globally, the total, atmosphere and ocean meridional energy transport anomalies for the experiments, relative to NoAero, are shown in Fig. 7. In the NET and SET experiments, the cooling of the northern/southern extratropics leads to energy transport anomalies further towards the tropics, with total transports peaking in both cases near the equator. The response of the atmospheric circulation, and tropical precipitation, is modulated by the split in energy transport changes between the atmosphere and ocean. Near the equator, the response in the atmosphere is greater than the ocean in both the NT and ST cases, whereas the relatively damped tropical precipitation response in the NET and SET experiments can be associated with the greater role of ocean energy transport anomalies in the tropics in those experiments. In the NET experiments, a relatively small total meridional energy transport anomaly occurs in the 1AOD case as the more modest TOA energy anomaly is largely absorbed in the northern latitudes, increasing temperature there (not shown).

Figure 8 shows the energy transport anomalies in the ocean for the 4AOD experiments with the response decomposed into the Atlantic, Pacific and (North) Indian Oceans. In the NET experiment, it is clear that the dominant response in the ocean is in the Atlantic as the AMOC increases in response to the cooling of the northern high latitudes. The ocean energy transport response becomes more dominant from the 2AOD to 4AOD case such that the tropical precipitation response between the two experiments is relatively small compared to the difference in forcing (see Fig. 2b). In the SET experiment, the response of the ocean is the dominant term in the 1AOD and 2AOD cases (Fig. 7b), which can be associated with the muted response in tropical precipitation in those experiments (see Fig. 2d), with a stronger atmospheric teleconnection only occurring in the 4AOD experiment. In the SET experiments, the ocean response is dominated by an increase in energy transport in the Pacific, with relatively little increase in tropical-extratropical energy transport in the Atlantic (Fig. 8b). Deser et al. (2015) and Tomas et al. (2016) have previously shown, in experiments investigating the response to a reduction in Arctic sea ice, that the ocean is crucial in modulating the global response to changes in the Arctic and that the AMOC reduces in

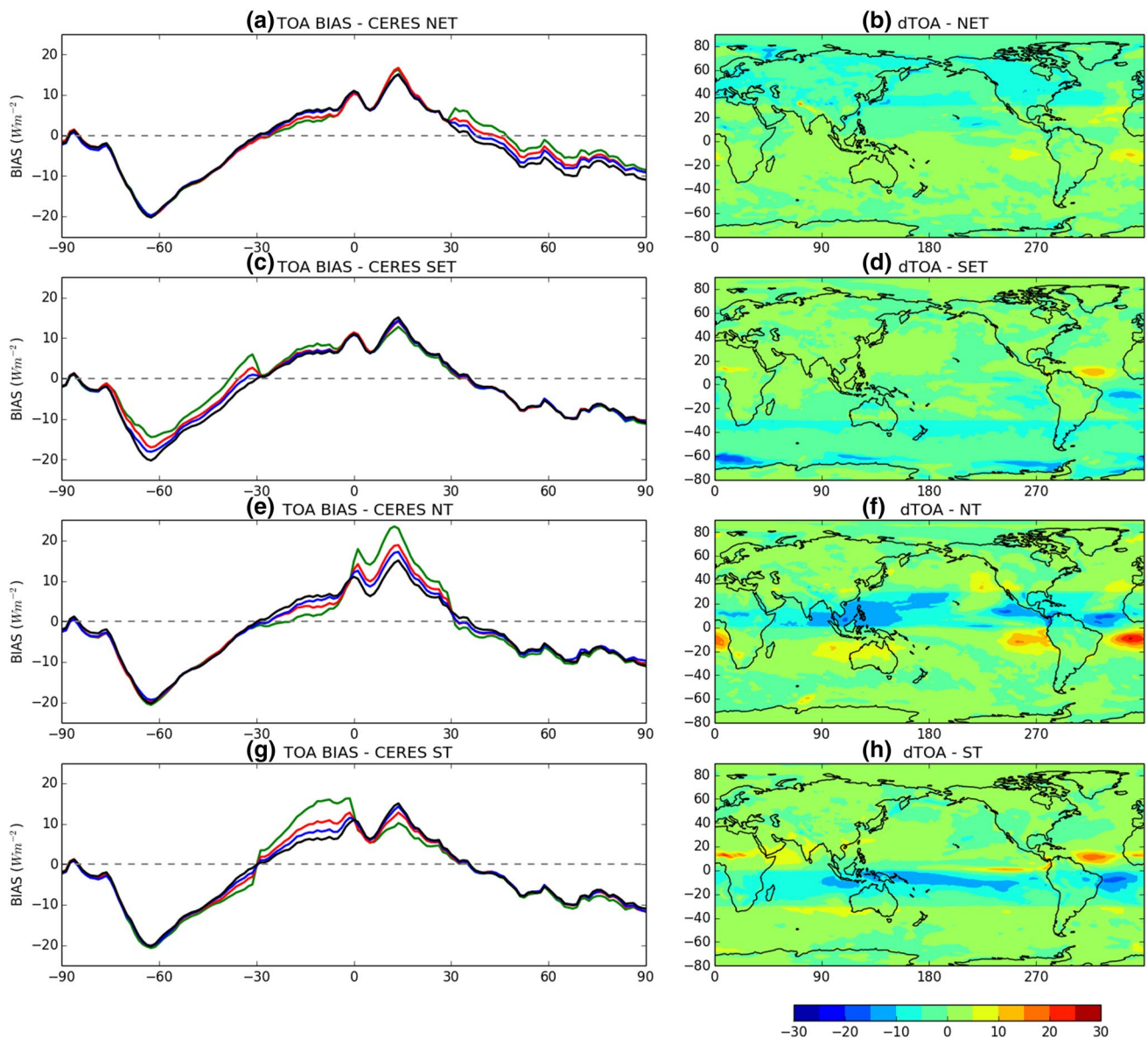


Fig. 5 **a, c, e, g** Top of atmosphere net radiation biases (W m^{-2} , upwards as positive) relative to CERES for the four experiments. The black line shows the NoAero simulation with the blue, red and green

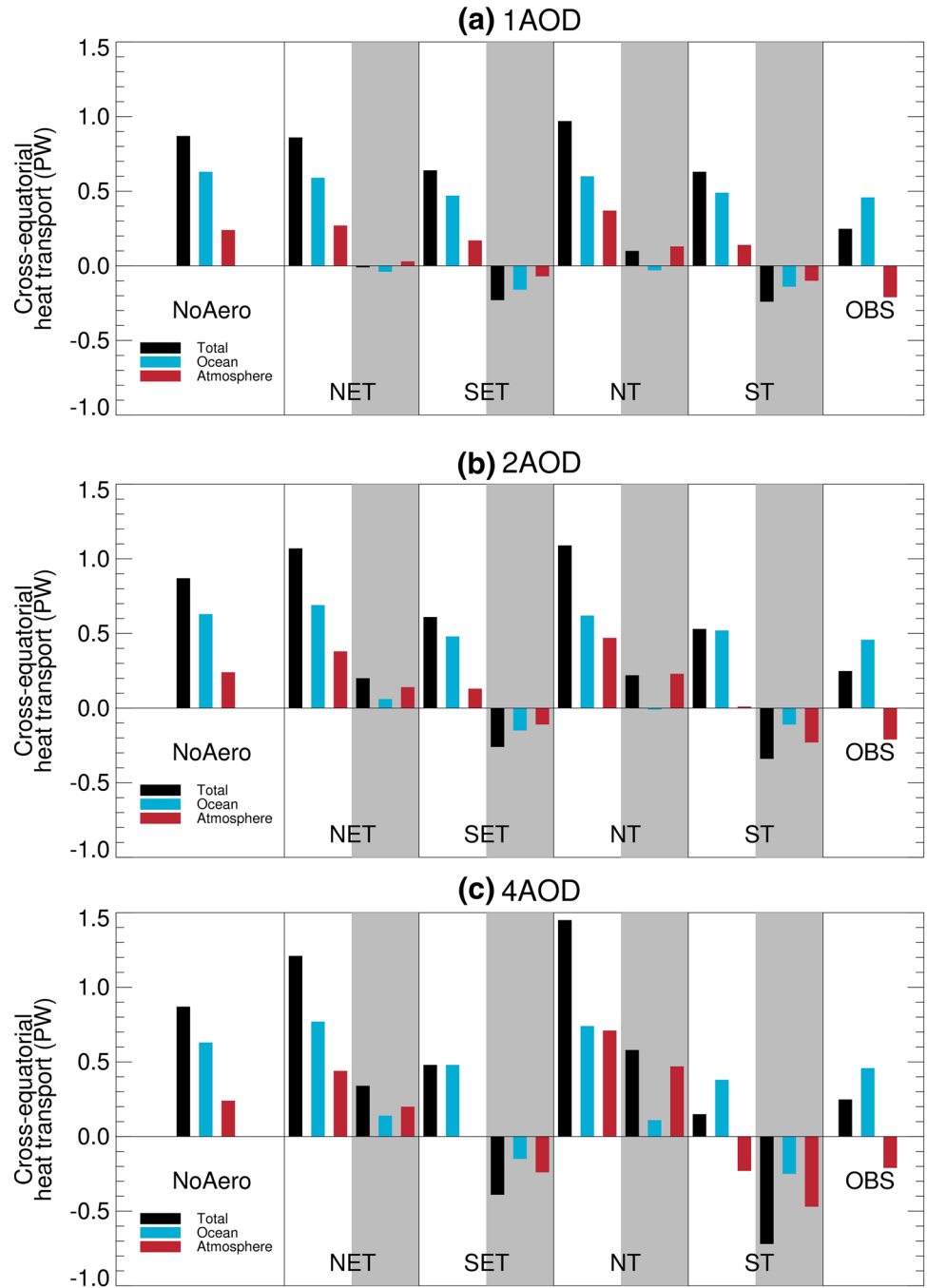
lines showing the 1, 2 and 4AOD experiments, respectively. **b, d, f, h** Top of atmosphere net radiation (W m^{-2} , downwards as positive) anomalies in the 4AOD experiments relative to the NoAero simulation

response to Arctic warming—an equivalent response to that found here, where the AMOC increases as the Arctic cools. This can be contrasted with the largely Pacific energy transport response in the SET experiment. Such a response was also observed in both Kay et al. (2016) and Hawcroft et al. (2016), where the Southern Ocean was cooled and tropical-extratropical energy transport in the Pacific increased, and is further discussed in Sect. 3.8.

In the NT and ST experiments, the maximum energy transport anomalies are situated around the equator (Fig. 7), where the local response to the TOA anomalies is to induce

an energy transport into the hemisphere that has been cooled. The response in the atmosphere at the equator is relatively linear in both cases, as it increases proportionately with forcing and explains the comparable response in tropical precipitation (see Fig. 2f, h). At the poleward flank of the forcing (30N and 30S) anomalies of opposite sign occur which are due to energy transport into the anomalously cooler tropical band from the mid-latitudes. In the ocean, the peak response is observed around 5° rather than at the equator itself. In both the NT and ST experiments, it is the Pacific that plays the most significant role in the ocean

Fig. 6 Cross-equatorial energy transport in the atmosphere (red), ocean (blue) and total (black, all in PW) for the NoAero and **a** 1AOD, **b** 2AOD and **c** 4AOD experiments and from observations (OBS). In each panel, the absolute values are shown for all datasets with the anomaly from the NoAero case to each of the perturbed experiments shown with a grey background



energy transport response (Fig. 8c, d). In both the NT and ST cases, the atmospheric circulation response around the equator generates an anomalous meridional wind stress which impacts the sub-tropical cells in the Pacific (Fig. 4d, e). In the NT case, the northward CET anomaly in the atmosphere is associated with a southward surface wind stress anomaly as the southern branch of the Hadley circulation weakens and the South Pacific Convergence Zone (SPCZ) intensifies (Fig. 4d). In the northern hemisphere, this slows the sub-tropical cell circulation and intensifies it in the southern

hemisphere (not shown). The opposite is true in the ST case, with a reduction in the SPCZ intensity and an increase in northward flow across the equator (Fig. 4e). At the equator itself, the ocean CET response in the Pacific in both cases is a direct response to the anomalous cross-equatorial wind stresses. In the SET experiment, the sub-tropical cells intensify (not shown) as the Pacific increases southward energy transport to the anomalously cool extratropics, similar to the response shown in Hawcroft et al. (2016) Figure 8, and further discussed in Sect. 3.8. The tropical atmospheric

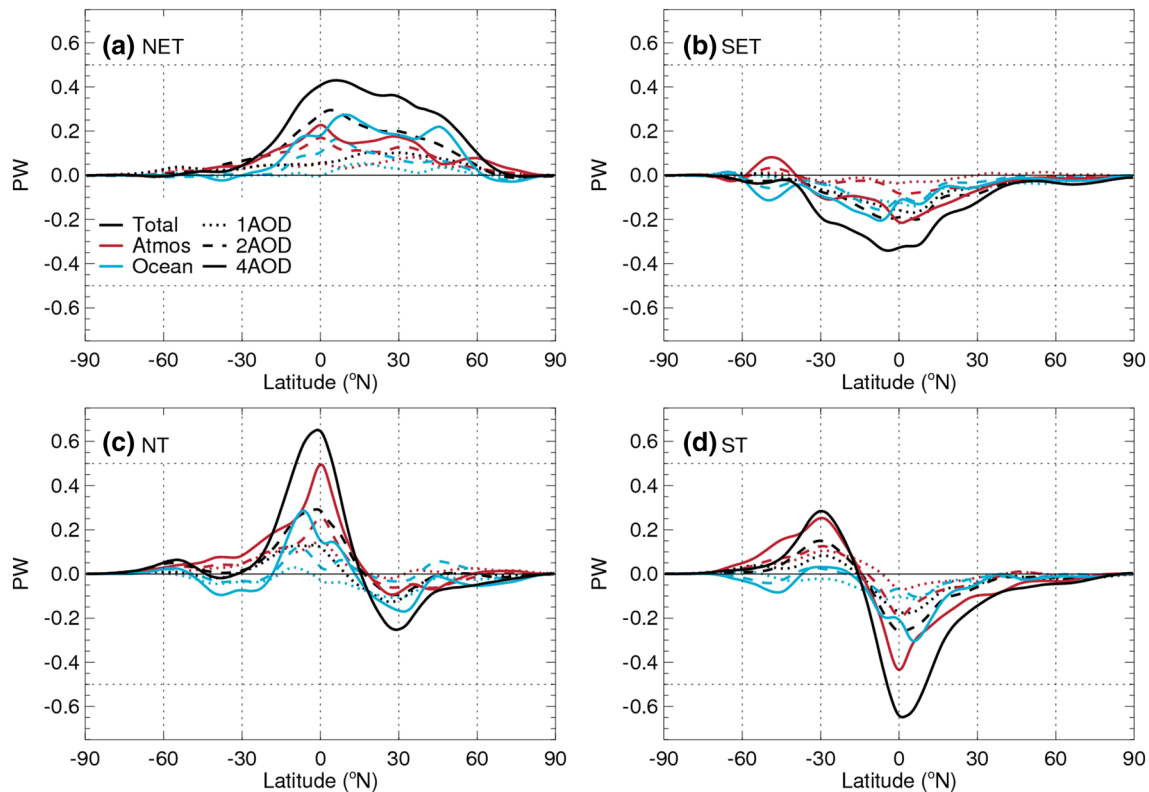


Fig. 7 Meridional energy transport anomalies (PW) in the **a** NET, **b** SET, **c** NT and **d** ST experiments relative to the NoAero experiment. In each panel, total (black), ocean (blue) and atmosphere (red)

energy transport are shown for the 1AOD (dotted), 2AOD (dashed) and 4AOD (solid) cases

response in each of these experiments is therefore dependent on the latitude of the forcing applied to the model, since the tropical teleconnection is a function of both the partitioning between atmosphere and ocean of the total response and also the basin in which the ocean response occurs.

3.7 Energy budget and dynamical response

In spite of the differences in circulation response to the differential forcings, a clear demonstration of the atmospheric CET-tropical precipitation relationship is shown in Fig. 9a, where a significant relationship ($> 99.9\%$, $R = -0.98$) between atmospheric CET (CETA) and tropical precipitation asymmetry (PAI) is shown, with a similarly strong relationship where the different metric of tropical precipitation centroid is used (Fig. 9b). It is notable that this holds in spite of the large anomalies imposed at and near the equator in the NT and ST experiments, which induce a near step-function in TOA net radiation at the equator (Fig. 1d, e), and that the linear fit does not pass through the observations. As discussed above, the ST 4AOD simulation has similar CETA to observations but with too much precipitation in the northern tropics (Fig. 2g)—the precipitation distribution remains too asymmetric compared to observations even with corrected

CETA. Adam et al. (2016) show a strong relationship ($R = -0.85$) between CETA and PAI in CMIP5 models and it is of interest to note that in spite of the idealised nature of the experiments shown here, the relationship is considerably closer between the two variables. This perhaps suggests structural differences between models may mean they are unable to sample the same space as each other as a result of fundamental structural differences and, more importantly, observations, even if the energy transports are improved or fully corrected.

Bischoff and Schneider (2016) show, using a series of slab ocean aquaplanet experiments where the net energy input (NEI) to the atmosphere is varied, that where NEI at the equator is negative, DI states occur in their experiments and that the asymmetry of tropical precipitation and the latitude of the ITCZ varies with increased asymmetry of NEI between the hemispheres. In experiments with negative NEI at the equator and a DI, as the atmosphere of one hemisphere has increased NEI, the ITCZ branch in that hemisphere intensifies and moves polewards as the opposite hemisphere's ITCZ weakens and moves equatorwards. Here, in a fully coupled GCM, we observe some similarities. The NEI near the equator remains negative in all experiments (Fig. 10) and NEI increases where aerosols are included

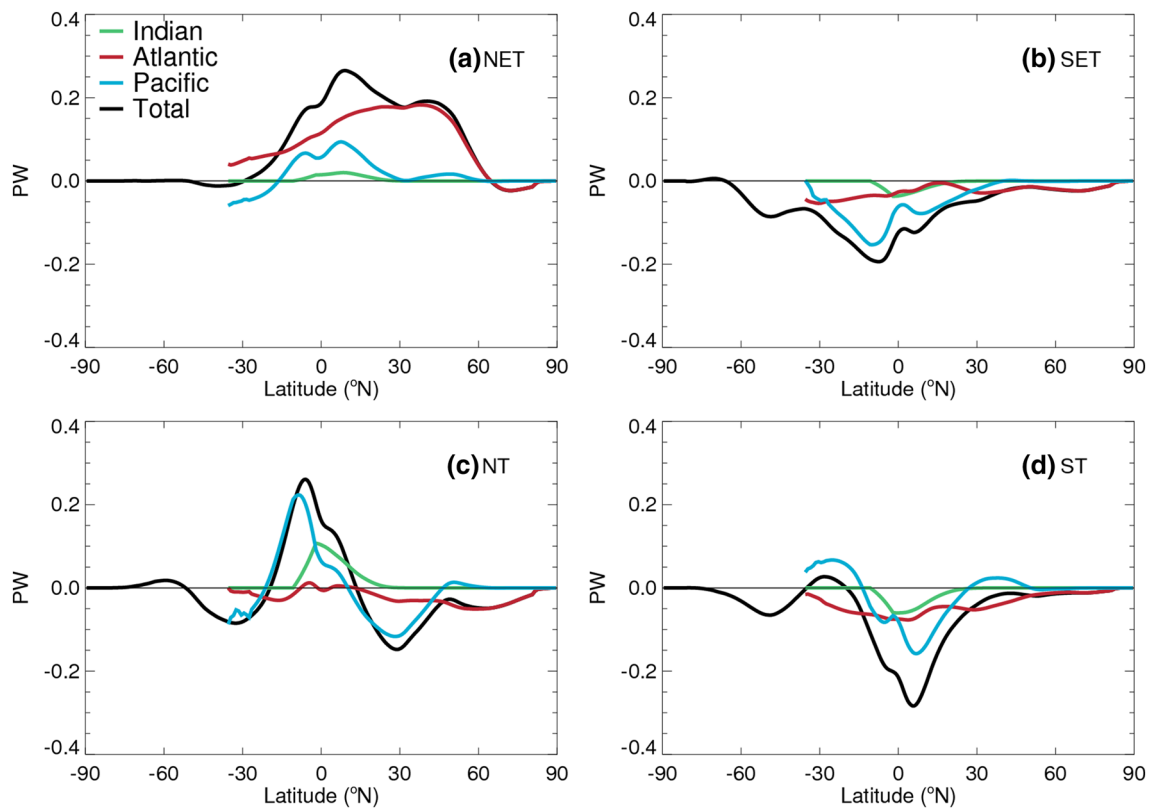


Fig. 8 Meridional ocean energy transport anomalies (PW) in the **a** NET, **b** SET, **c** NT and **d** ST 4AOD experiments relative to the NoAero experiment. In each panel, total (black), Pacific (blue), Atlantic (red) and Indian (green) Ocean transport anomalies are shown

and where the ITCZ intensity and associated cloud radiative heating increases (see Fig. 2). The latitude at which the most intense band of the ITCZ precipitation (P_{max}), in either hemisphere, is situated does not alter materially, as seen in the monotonic poleward migration with increased hemispherically asymmetric NEI in the experiments of Bischoff and Schneider (2016), though the centroid of the precipitation (P_{cent} defined as the median latitude of the zonal mean precipitation between 20S and 20N) adjusts, as in the experiments of Bischoff and Schneider (Fig. 9b). This relationship has previously been demonstrated in coupled models (Donohoe et al. 2013), where the CMIP3 models were analysed. The results in this study further show that the relationship between atmospheric CET and hemispheric biases in tropical precipitation are robust, even in idealised simulations where strong energy perturbations are imposed and where the underlying model is a full GCM with continents, orography and a dynamical ocean modulating the response of the model climate.

The bimodality of tropical precipitation, switching from one preferred mean ITCZ location to another, is observed in the seasonal cycle of both coupled models and observations (Donohoe et al. 2013) and is also seen in the experiments analyzed here (Fig. 11), with changes in the intensity of the

northern/southern hemisphere bands clearly evident but little adjustment in the seasonal cycle, the timing of the migration of the core of the zonal mean precipitation between hemispheres and the latitude of those bands.

Donohoe et al. (2013) found that in CMIP3 models with an annual mean P_{cent} that was further north/south, the maximum/minimum latitudes of the ITCZ during the annual cycle were further north/south, rather than the intensity (i.e. P_{max}) changing, but the latitude of the most intense precipitation remaining in a similar location, as seen in Fig. 11. This implies that the physical biases in models which determine the absolute latitude of P_{max} , in both the annual mean and during the annual cycle, may not be the same as those governing P_{cent} , the behaviour of which has been shown to be closely tied to atmospheric CET in this study and others, highlighting the need to increase understanding what processes govern the latitude of P_{max} in climate models and observations.

Haywood et al. (2016) showed that where a hemispherically uniform perturbation was imposed in the southern hemisphere, tropical precipitation asymmetry was greatly improved and that tropical SST gradients also responded to the differential energy input to the two hemispheres. In those experiments, the cross-equatorial SST gradient increased,

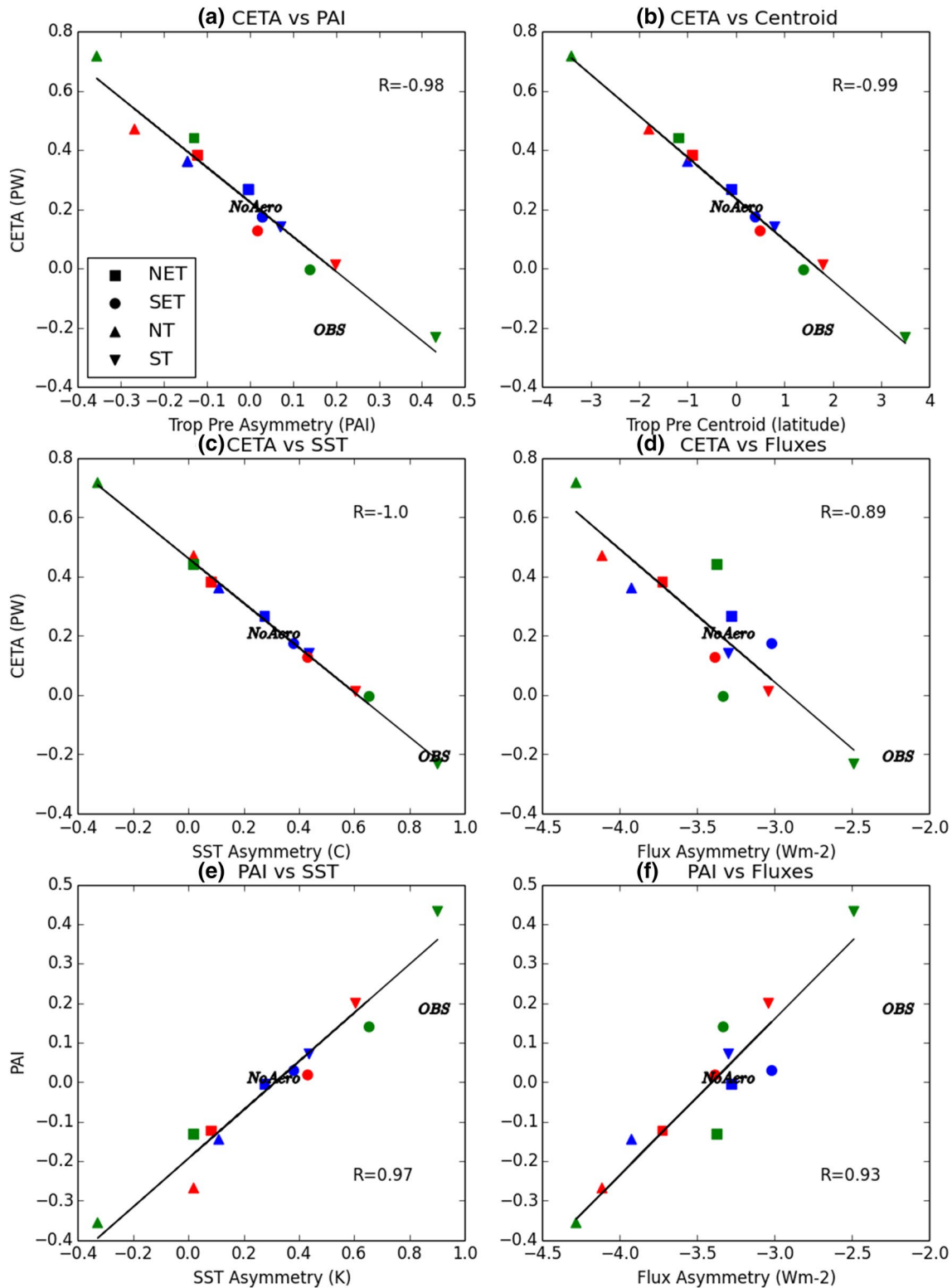


Fig. 9 Cross-equatorial energy transport in the atmosphere (CETA) and **a** tropical precipitation asymmetry (PAI) for the NoAero and 1AOD (blue), 2AOD (red) and 4AOD (green) experiments, **b** the centroid of tropical precipitation (degrees), **c** tropical SST asymmetries (K), **d** surface flux asymmetries ($W m^{-2}$). PAI and **e** tropical SST asymmetries and **f** surface flux asymmetries. The precipitation (P)

asymmetry is calculated as $P_{0--20N} - P_{0--20S} / P_{20S--20N}$. The centroid is calculated as the median latitude of the integrated zonal mean precipitation between 20S and 20N. SST and surface flux asymmetries are the difference between 0–20N and 0–20S. Observations (OBS) are taken from CERES, GPCP, OISST and the OAFflux dataset. Surface fluxes are ocean only

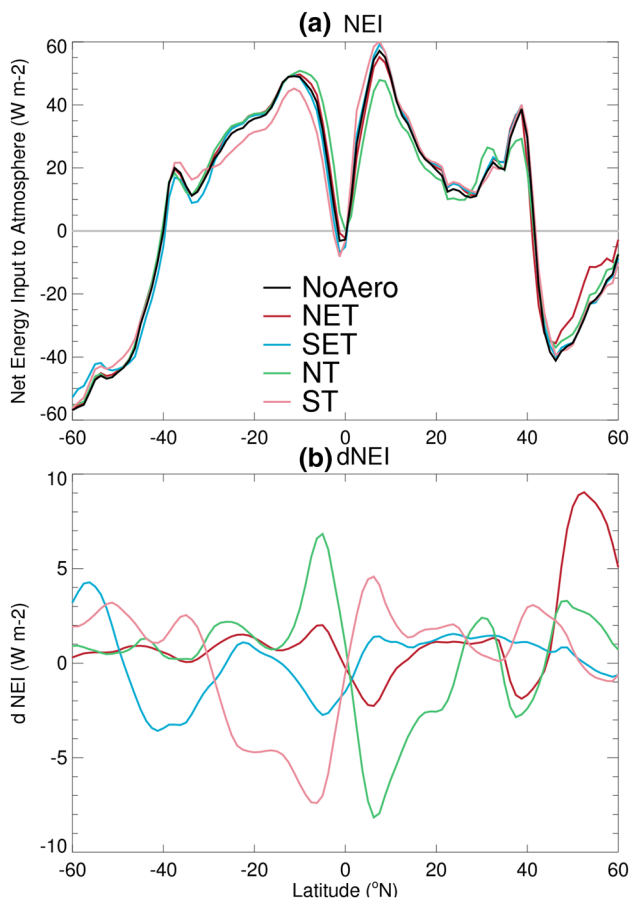


Fig. 10 Net energy input (NEI, W m^{-2}) to the atmosphere in the NoAero experiment and the four 4AOD experiments shown as **a** absolute values and **b** anomalies from the NoAero experiment

with the southern hemisphere cooling, and this corresponded to a northward shift in tropical precipitation. The same relationship is shown in Fig. 9c, where tropical SST asymmetries respond in the same linear fashion to the TOA anomalies as CETA and also PAI (e). Previous studies have noted the link between Sahelian precipitation and tropical SST gradients (e.g. Zeng 2003; Folland et al. 1986) and it has further been argued that this behaviour may be linked to (northern hemisphere) anthropogenic aerosol emissions (Ackerley et al. 2011; Booth et al. 2012), indicating that this coupled response in the observed climate system may have occurred through similar mechanisms to those explored in this study. This implies a strong role for atmospheric model biases, particularly in the tropics, driving the DI biases seen in many models. Xiang et al. (2017) have recently argued that the biases in tropical SSTs that are closely coupled with DI biases in the CMIP5 models may be strongly linked to tropical surface flux biases. In Fig. 9 the relationships between the tropical surface net fluxes and CETA (d) and PAI (f) are shown. The relationships here are not as strongly coupled as CETA/PAI/SST (a, c, e), though still highly

significant. It may be that the slightly weaker relationship here is associated with the circulation anomalies induced at the equator in these experiments (see Fig. 4) as cross-equatorial zonal mean vertically integrated moisture fluxes are relatively noisy in the experiments with smaller CETA responses (not shown), moving moisture sourced from one hemisphere into the other before it precipitates and decreasing the robustness of this relationship. All these metrics, however, show the strong connections between the energy budget, tropical precipitation, SSTs and surface fluxes and indicate that atmospheric model biases in the tropics can play a major role in the DI and CETA biases seen in coupled models.

3.8 Southern ocean cooling and teleconnections

In this study, the response to the SET experiments is of particular interest given previous work examining the tropical response to a cooling of the Southern Hemisphere, especially the mid to high latitudes. In Haywood et al. (2016), a cooling of the whole southern hemisphere was imposed on HadGEM2-ES (the model used here), which induced a similar step-function in TOA net radiation to that in the ST/NT experiments in this study (Fig. 1d, e). The dramatic improvements in tropical precipitation in Haywood et al. (2016) can therefore be interpreted as a local circulation response to this anomaly, similar to the improvement in CET and precipitation seen in the ST 2AOD and 4AOD experiments, underscoring the potential benefits to the tropical climatology of models of reducing biases in these first order metrics of model fidelity. In contrast, Kay et al. (2016) and Hawcroft et al. (2016) found that an increase in albedo in the Southern Ocean (where the bias reductions were centred on $\sim 65\text{S}$) had little impact on tropical precipitation, even though the forcings were in excess of 10 Wm^{-2} , which is similar in magnitude to the 4AOD experiments (Fig. 1). The SET 4AOD experiment resulted in a northward shift of the ITCZ and reduction of the DI bias (Fig. 2d, green line) as part of the energy transport response in the tropics was via a southward energy transport anomaly in the atmosphere (Fig. 7b, solid red line). Further, Mechoso et al. (2016), applying a forcing between 30 and 60S in two models, found very little ITCZ response in NorESM but a northward shift of the ITCZ in the UCLA GCM. Though some of these differences are likely associated with differing model background states and biases, they are also (at least in HadGEM2-ES) associated with experimental design.

In Fig. 12, zonal mean eastward winds are shown for the NoAero and the SET 4AOD experiments and for an equivalent experiment, SWex4, and the comparable historical (CLIM) simulation in HadGEM2-ES, both taken from Hawcroft et al. (2016), where the cooling of the southern extratropics is focussed on 60–90S. The anomalies in Fig. 12

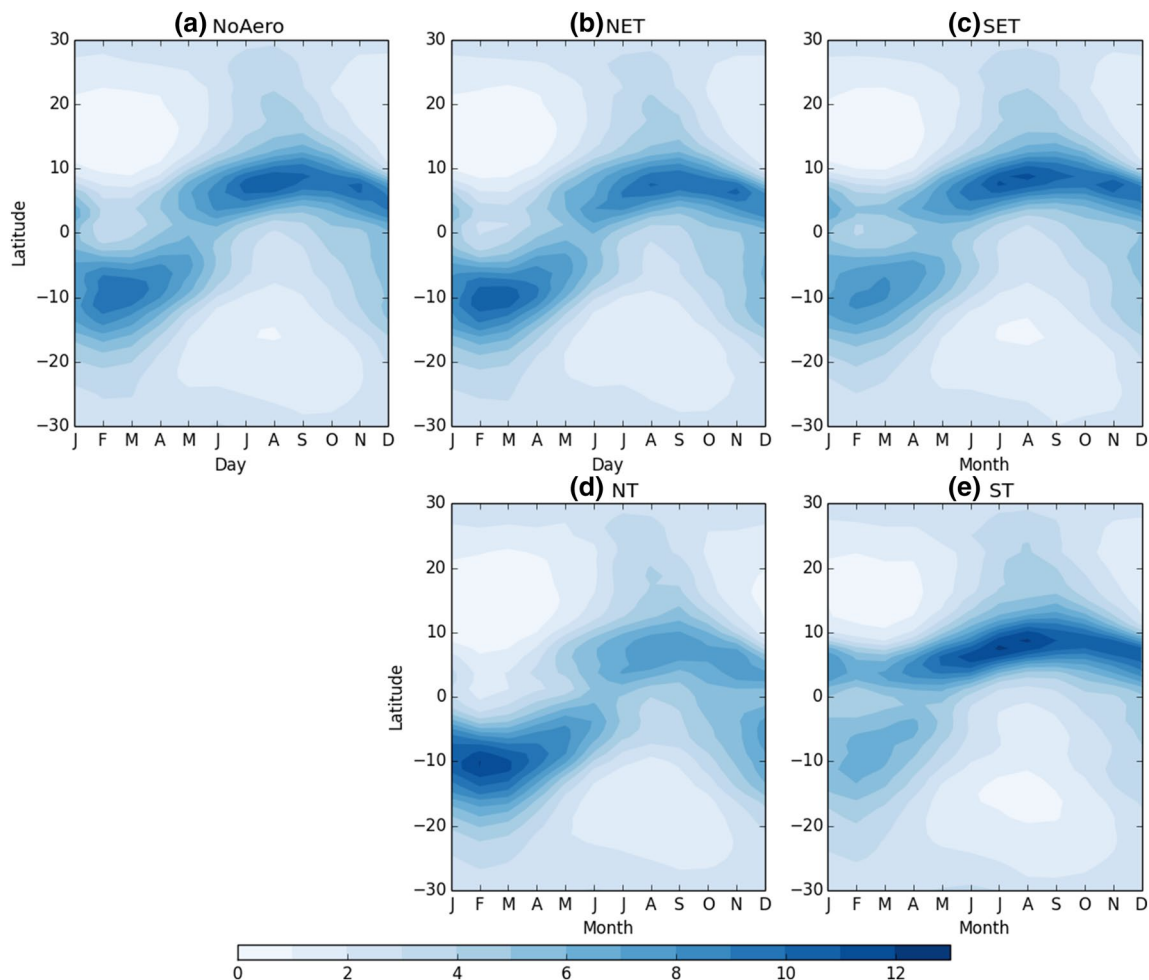


Fig. 11 Annual cycle of zonal mean precipitation (mm day^{-1}) for the NoAero and 4AOD experiments

are with respect to the companion control case—NoAero/SET and CLIM/SWex4. The differences in the two responses show the sensitivity of the circulation response to the latitude of the forcing. In the SET simulation, the northward boundary of the cooling is 30S, leading to an increase in the meridional temperature and baroclinic gradient through the sub-tropics and a northward shift in the core of the jet. The most intense westerlies (at 60S) weaken as the surface temperature gradient reduces through this region (not shown).

In contrast, in the SWex4 simulation, the strongest cooling is restricted to higher latitudes, increasing the surface temperature and baroclinic gradient (not shown) in the region where the westerlies are already at their strongest in the control experiment. This leads to an intensification of the existing circulation without a change in the latitude of the low level winds. In SET, the northward expansion of the region of stronger westerlies slightly increases surface wind stress at 40S (Fig. 4c), though these anomalies are far smaller than those at 60S in Hawcroft et al.

(2016). These differences can be related to the differential response in ocean/atmosphere energy transport in the two simulations (Figure 7b and Figure 6 of Hawcroft et al. (2016)). In Hawcroft et al. (2016), much of the tropical energy transport changes were achieved in the Pacific as the sub-tropical cells intensified as part of wider changes in the Pacific circulation, with little response in the Atlantic. In SET, southward ocean energy transport anomalies in the Pacific are less pronounced (Fig. 8b), leading to an increased southward anomaly in atmospheric CET (Fig. 6c) and northward shift of the ITCZ (Fig. 2b). It may therefore be that some of the differences in Mechoso et al. (2016) compared to Kay et al. (2016) and Hawcroft et al. (2016) could be connected to similar circulation anomalies associated with experimental design. Relatedly, the latitude of albedo and radiation biases across climate models may impact on their tropical circulation through similar sensitivities.

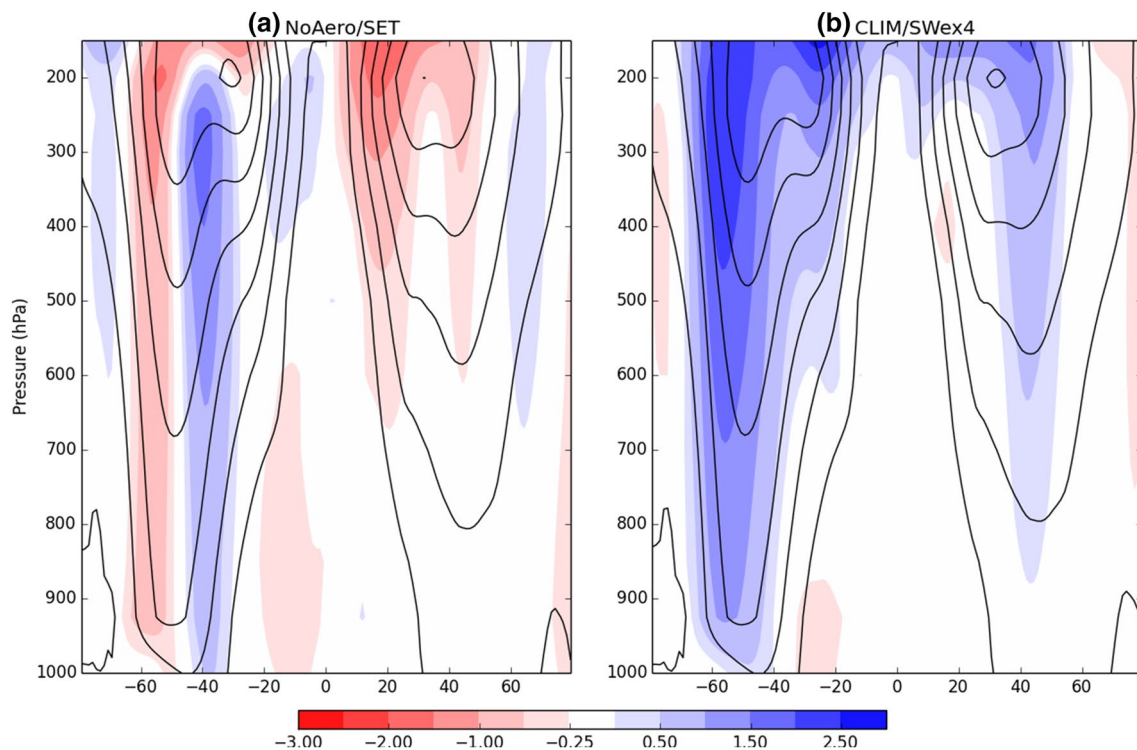


Fig. 12 Zonal mean eastward wind anomalies (m s^{-1}) for the **a** SET and **b** the SWex4 experiment from Hawcroft et al. (2016). Anomalies are shown from the **a** NoAero experiment and **b** CLIM experiment

in Hawcroft et al. (2016), with the **a** NoAero and **b** CLIM values as unfilled contours at 5 m s^{-1} intervals with 0 m s^{-1} as the lowest visible contour

4 Conclusions

This study has investigated the differential response to imposing a cooling in defined latitude bands in a fully coupled climate model. Building on previous work looking at teleconnections, energy transport and the impact of extratropical climate anomalies on the tropics, particularly tropical precipitation, a spread of behaviour has been observed. Where the tropics is cooled directly via an increase in stratospheric aerosol, a direct circulation response occurs, with increased cross-equatorial energy transport into the cooled hemisphere and a shift of tropical precipitation into the warmer hemisphere, as expected from previous studies examining both observations and models (e.g. Donohoe et al. 2013; Hwang and Frierson 2013; Schneider et al. 2014; Loeb et al. 2015; Bischoff and Schneider 2016; Adam et al. 2016). Where the cooling is applied to the extratropics, the tropical response is modulated by the nature of the teleconnection pathway since meridional energy transport adjustments can occur in the atmosphere or ocean, and in different ocean basins. Sensitivity to experimental design when interrogating these issues has also been highlighted.

The main findings of this study are as follows:

- The response of the tropical atmosphere to hemispherically asymmetric energy perturbations in a coupled model is highly dependent on the latitude of the forcing, with ocean and atmosphere circulation responses to extratropical perturbations modulating the tropical response. Tropical atmosphere responses are damped where ocean circulation anomalies achieve much of the energy transport response in a model.
- The relationship between tropical precipitation asymmetry and cross-equatorial atmospheric energy transport is very closely coupled, as is the relationship between both these indices and tropical SST asymmetry.
- The structural biases in the model which lead to biases in cross-equatorial energy transport are very resistant to change—it takes a forcing equivalent to twice the stratospheric aerosol optical depth after the Pinatubo eruption ($\sim 10\text{ Wm}^{-2}$) over the southern tropics to correct these cross-equatorial energy transport biases.
- Biases in the tropical climate in models, future projections of the tropical climate from models and the response of climate models to idealised forcing may all have dependence on the particular latitude of any albedo/energy budget biases or forcing. Understanding the causes and impacts of such biases or responses to

forcing is therefore an important component of model development.

The outcomes of this study may be considered preliminary since they are the results of experiments using a single model, with the energy perturbations imposed in the stratosphere only. In defence of the latter criticism, the results shown here can be compared and interpreted with reference to other experiments using the same model where the ocean surface (Hawcroft et al. 2016), stratospheric aerosol and cloud radiative properties (Haywood et al. 2016) have been altered, with results that indicate a qualitatively consistent response to forcings in different latitudes irrespective of how those forcings are applied. In terms of model dependence, other studies investigating the response to idealised brightening of the Southern Ocean have shown some differences in response (Kay et al. 2016; Mechoso et al. 2016), though these issues may also be partly associated with experimental design (as discussed in Sect. 3.8).

It is clear that any large scale, zonal mean bias in the energy budget of a climate model may have remote impacts and, when considering future climate projections under a warming scenario, the tropical response of a model will be related to the extratropical response, though this study highlights the uncertainty in those teleconnections if there are underlying biases in any given model. For example, Arctic amplification (Holland and Bitz 2003) both determines and is modulated by the climate response at lower latitudes (Deser et al. 2015; Tomas et al. 2016) so any biases in the Arctic and the circulation anomalies associated with high latitude warming may have implications for the global climate response. The persistence of the DI problem through generations of climate models (Zhang et al. 2015) and the potential impact of such biases on the response of models to warming is also clearly an issue when considering future projections and is closely related to tropical atmospheric energy transport biases.

In order to increase confidence in future projections of climate change and reduce the spread of response across models, it is essential that the sources and controls on these large scale biases are understood and reduced. As part of broader efforts to understand the sources of these biases and the spread of model behaviour, the ongoing Extratropical-Tropical Interaction Model Intercomparison Project (ETIN-MIP) is underway, applying a series of idealised forcings to multiple GCMs in order to probe the nature and the spread of model response. The present authors are also investigating the behaviour of a perturbed physics ensemble (PPE) of more recent version of the Hadley Centre model in order to investigate the physical processes which may play particularly important roles in these large scale biases.

Acknowledgements MKH, MC and JMH were supported by the Natural Environment Research Council/Department for International Development via the Future Climates for Africa (FCFA) funded project 'Improving Model Processes for African Climate' (IMPALA, NE/M017265/1). JMH and AJ were supported by the Joint UK BEIS/Defra Met Office Hadley Centre Climate Programme (GA01101). The authors thank the editor and reviewer for useful comments which improved this manuscript.

Open Access This article is distributed under the terms of the Creative Commons Attribution 4.0 International License (<http://creativecommons.org/licenses/by/4.0/>), which permits unrestricted use, distribution, and reproduction in any medium, provided you give appropriate credit to the original author(s) and the source, provide a link to the Creative Commons license, and indicate if changes were made.

References

- Ackerley D, Booth BB, Knight SH, Highwood EJ, Frame DJ, Allen MR, Rowell DP (2011) Sensitivity of twentieth-century sahel rainfall to sulfate aerosol and co2 forcing. *J Clim* 24(19):4999–5014
- Adam O, Schneider T, Briant F, Bischoff T (2016) Relation of the double-ITCZ bias to the atmospheric energy budget in climate models. *Geophys Res Lett* 43(14):7670–7677 (2016GL069465)
- Adler RF, Huffman GJ, Chang A, Ferraro R, Xie PP, Janowiak J, Rudolf B, Schneider U, Curtis S, Bolvin D et al (2003) The version-2 global precipitation climatology project (gpcp) monthly precipitation analysis (1979–present). *J Hydrometeorol* 4(6):1147–1167
- Balmaseda MA, Mogensen K, Weaver AT (2013) Evaluation of the ecmwf ocean reanalysis system oras4. *Q J R Meteorol Soc* 139(674):1132–1161
- Bellucci A, Gualdi S, Navarra A (2010) The double-ITCZ syndrome in coupled general circulation models: the role of large-scale vertical circulation regimes. *J Clim* 23(5):1127–1145
- Bischoff T, Schneider T (2014) Energetic constraints on the position of the intertropical convergence zone. *J Clim* 27(13):4937–4951
- Bischoff T, Schneider T (2016) The equatorial energy balance, ITCZ position, and double-ITCZ bifurcations. *J Clim* 29(8):2997–3013
- Bodas-Salcedo A, Williams KD, Ringer MA, Beau I, Cole JN, Dufresne JL, Koshiro T, Stevens B, Wang Z, Yokohata T (2014) Origins of the solar radiation biases over the southern ocean in cfmip2 models*. *J Clim* 27(1):41–56
- Booth BB, Dunstone NJ, Halloran PR, Andrews T, Bellouin N (2012) Aerosols implicated as a prime driver of twentieth-century north atlantic climate variability. *Nature* 484(7393):228–232
- Chiang JC, Bitz CM (2005) Influence of high latitude ice cover on the marine intertropical convergence zone. *Clim Dyn* 25(5):477–496
- Collins W, Bellouin N, Doutriaux-Boucher M, Gedney N, Halloran P, Hinton T, Hughes J, Jones C, Joshi M, Liddicoat S et al (2011) Development and evaluation of an earth-system model-hadgem2. *Geosci Model Dev* 4(4):1051–1075
- Cvijanovic I, Chiang JC (2013) Global energy budget changes to high latitude north atlantic cooling and the tropical ITCZ response. *Clim Dyn* 40(5–6):1435–1452
- Dee D, Uppala S, Simmons A, Berrisford P, Poli P, Kobayashi S, Andrae U, Balmaseda M, Balsamo G, Bauer P et al (2011) The era-interim reanalysis: configuration and performance of the data assimilation system. *Q J R Meteorol Soc* 137(656):553–597
- Deser C, Tomas RA, Sun L (2015) The role of ocean-atmosphere coupling in the zonal-mean atmospheric response to arctic sea ice loss. *J Clim* 28(6):2168–2186

- Donohoe A, Marshall J, Ferreira D, Mcgee D (2013) The relationship between itcz location and cross-equatorial atmospheric heat transport: from the seasonal cycle to the last glacial maximum. *J Clim* 26(11):3597–3618
- Folland C, Palmer T, Parker D (1986) Sahel rainfall and worldwide sea temperatures, 1901–85. *Nature* 320(6063):602–607
- Frierson DM, Hwang YT (2012) Extratropical influence on itcz shifts in slab ocean simulations of global warming. *J Clim* 25(2):720–733
- Gregory J, Ingram W, Palmer M, Jones G, Stott P, Thorpe R, Lowe J, Johns T, Williams K (2004) A new method for diagnosing radiative forcing and climate sensitivity. *Geophys Res Lett* 31(3):205. <https://doi.org/10.1029/2003GL018747>
- Hansen J, Lacis A, Ruedy R, Sato M (1992) Potential climate impact of mount pinatubo eruption. *Geophys Res Lett* 19(2):215–218
- Hawcroft M, Haywood JM, Collins M, Jones A, Jones AC, Stephens G (2016) Southern ocean albedo, inter-hemispheric energy transports and the double ITCZ: global impacts of biases in a coupled model. *Clim Dyn* 48:2279–2295
- Haywood JM, Jones A, Dunstone N, Milton S, Vellinga M, Bodas-Salcedo A, Hawcroft M, Kravitz B, Cole J, Watanabe S et al (2016) The impact of equilibrating hemispheric albedos on tropical performance in the hadgem2-es coupled climate model. *Geophys Res Lett* 43:395–403
- Hofmann DJ (1987) Perturbations to the global atmosphere associated with the el chichon volcanic eruption of 1982. *Rev Geophys* 25(4):743–759
- Holland MM, Bitz CM (2003) Polar amplification of climate change in coupled models. *Clim Dyn* 21(3–4):221–232
- Hwang YT, Frierson DM (2013) Link between the double-intertropical convergence zone problem and cloud biases over the southern ocean. *Proc Natl Acad Sci* 110(13):4935–4940
- Kang SM, Held IM, Frierson DM, Zhao M (2008) The response of the itcz to extratropical thermal forcing: Idealized slab-ocean experiments with a gcm. *J Clim* 21(14):3521–3532
- Kato S, Loeb NG, Rose FG, Doelling DR, Rutan DA, Caldwell TE, Yu L, Weller RA (2013) Surface irradiances consistent with ceres-derived top-of-atmosphere shortwave and longwave irradiances. *J Clim* 26(9):2719–2740
- Kay JE, Wall C, Yettella V, Medeiros B, Hannay C, Caldwell P, Bitz C (2016) Global climate impacts of fixing the southern ocean shortwave radiation bias in the community earth system model (cesm). *J Clim*. <https://doi.org/10.1175/JCLI-D-15-0358.1>
- Li JL, Waliser D, Stephens G, Lee S, L'Ecuyer T, Kato S, Loeb N, Ma HY (2013) Characterizing and understanding radiation budget biases in cmip3/cmip5 gcms, contemporary gcm, and reanalysis. *J Geophys Res Atmos* 118(15):8166–8184
- Lin JL (2007) The double-itzc problem in ipcc ar4 coupled gcms: Ocean-atmosphere feedback analysis. *J Clim* 20(18):4497–4525
- Loeb NG, Wielicki BA, Doelling DR, Smith GL, Keyes DF, Kato S, Manalo-Smith N, Wong T (2009) Toward optimal closure of the earth's top-of-atmosphere radiation budget. *J Clim* 22(3):748–766
- Loeb NG, Kato S, Su W, Wong T, Rose FG, Doelling DR, Norris JR, Huang X (2012) Advances in understanding top-of-atmosphere radiation variability from satellite observations. *Surv Geophys* 33(3–4):359–385
- Loeb NG, Wang H, Cheng A, Kato S, Fasullo JT, Xu KM, Allan RP (2015) Observational constraints on atmospheric and oceanic cross-equatorial heat transports: revisiting the precipitation asymmetry problem in climate models. *Clim Dyn* 46:3239–3257
- Mechoso CR, Losada T, Koseki S, Mohino-Harris E, Keenlyside N, Casta-Tierno A, Myers TA, Rodriguez-Fonseca B, Toniazzo T (2016) Can reducing the incoming energy flux over the southern ocean in a cgm improve its simulation of tropical climate? *Geophys Res Lett* 43(20):11057–11063. <https://doi.org/10.1002/2016GL071150>
- NCAR (2014) National center for atmospheric research staff (eds). the climate data guide: Era-interim: derived components. <https://climatedataguide.ucar.edu/climate-data/era-interim-derived-components>, accessed: 2015-02-12
- Oueslati B, Bellon G (2015) The double itcz bias in cmip5 models: interaction between sst, large-scale circulation and precipitation. *Clim Dyn* 44(3–4):585–607
- Reynolds RW (2009) What's new in version 2. NOAA/NCDC Tech Note
- Reynolds RW, Smith TM, Liu C, Chelton DB, Casey KS, Schlax MG (2007) Daily high-resolution-blended analyses for sea surface temperature. *J Clim* 20(22):5473–5496
- Robock A (2000) Volcanic eruptions and climate. *Rev Geophys* 38(2):191–219
- Sato M, Hansen JE, McCormick MP, Pollack JB (1993) Stratospheric aerosol optical depths, 1850–1990. *J Geophys Res Atmos* 98(D12):22987–22994
- Schneider T, Bischoff T, Haug GH (2014) Migrations and dynamics of the intertropical convergence zone. *Nature* 513(7516):45–53
- Stephens GL, Hakuba MZ, Hawcroft M, Haywood JM, Behrangi A, Kay JE, Webster PJ (2016) The curious nature of the hemispheric symmetry of the earths water and energy balances. *Curr Clim Change Rep* 2(4):135–147
- Stocker T (2014) Climate change 2013: the physical science basis: Working Group I contribution to the Fifth assessment report of the Intergovernmental Panel on Climate Change. Cambridge University Press, Cambridge
- Tomas RA, Deser C, Sun L (2016) The role of ocean heat transport in the global climate response to projected arctic sea ice loss. *J Clim* 29(19):6841–6859. <https://doi.org/10.1175/JCLI-D-15-0651.1>
- Voigt A, Bony S, Dufresne JL, Stevens B (2014a) The radiative impact of clouds on the shift of the intertropical convergence zone. *Geophys Res Lett* 41(12):4308–4315
- Voigt A, Stevens B, Bader J, Mauritsen T (2014b) Compensation of hemispheric albedo asymmetries by shifts of the itcz and tropical clouds. *J Clim* 27(3):1029–1045
- Wielicki BA, Barkstrom BR, Harrison EF, Lee RB III, Louis Smith G, Cooper JE (1996) Clouds and the earth's radiant energy system (ceres): An earth observing system experiment. *Bull Am Meteorol Soc* 77(5):853–868
- Xiang B, Zhao M, Held I, J-C Golaz (2017) Predicting the severity of the spurious 'double ITCZ' problem in CMIP5 coupled models from AMIP simulations. *Geophys Res Lett* 44:1520–1527
- Yu L, Jin X, Weller RA (2008) Multidecade global flux datasets from the objectively analyzed air-sea fluxes (oafux) project: Latent and sensible heat fluxes, ocean evaporation, and related surface meteorological variables lisan yu. OAFux Project Tech Rep OA-2008-01 64pp 74
- Zeng N (2003) Drought in the sahel. *Science* 302(5647):999–1000
- Zhang GJ, Wang H (2006) Toward mitigating the double ITCZ problem in NCAR CCSM3. *Geophys Res Lett* 33(6):L06709. <https://doi.org/10.1029/2005GL025229>
- Zhang X, Liu H, Zhang M (2015) Double itcz in coupled ocean-atmosphere models: From cmip3 to cmip5. *Geophys Res Lett* 42(20):8651–8659